Semi-Deterministic vs. Genetic Algorithms for Global Optimization of Multichannel Optical Filters

Benjamin Ivorra, Bijan Mohammadi, Patrick Redont
Mathematics and Modelling Institute, University Montpellier II, 34095 Montpellier, France

Laurent Dumas
Jacques-Louis Lions Laboratory University of Paris VI, 75252 Paris, France

Olivier Durand
Alcatel CRC, 91460 Marcoussis, France

Abstract: A new global optimization algorithm is presented and applied to the design of high-channel-count multichannel filters based on sampled Fiber Bragg Gratings. We focus on the realization of particular designs corresponding to multichannel filters that consist of 16 and 38 totally reflective identical channels spaced 100 GHz. The results are compared with those obtained by a hybrid genetic algorithm and by the classical sinc method.

Keywords: global optimization; semi-deterministic algorithms; genetic algorithms; optical fiber devices; multiplexing.

1 INTRODUCTION

The use of new optical fiber devices in the telecommunication sector has known an important development in the last few years. Among them, Fiber Bragg Gratings (FBG) based devices represent an attractive alternative for applications such as multichannel filtering, multichannel optical add/drop multiplexing, multichannel dispersion compensation and multiwavelength laser sources. Focusing on this last domain, the FBG functionality is to ensure the choice of desired wavelengths by forming a step-tunable laser (Chow et al., 1996; Wei et al., 2000). It may be incorporated either in all-fiber structures such as erbium-doped fiber ring lasers or hybridized with an external Fabry-Perot cavity (Helmers et al., 2002). One way to perform their realization is to use sampled FBGs. Such filters are made of a spatial comb distribution of identical sampling gratings.

Pioneer works on this topic have reported results obtained with amplitude-only sampling through the writing of periodic transmitting and opaque regions inside the fiber core (Eggleton et al., 1994). The main drawback in this case is the sinc envelope of the spectral response due to the square index envelope of every transmitting region. The uniformity of the response is then limited to only a few nanometers. In order to overcome this non-uniformity, it was proposed to insulate the opaque regions with sets of interleaved amplitude-only sampling patterns for yielding interleaved groups of channels (Loh et al., 1999). However, a predictable number of peaks inside an overall square envelope is still difficult to reach in this case.

A lot of work was then performed for optimizing the sampling pattern either in amplitude (Ibsen et al., 1998) and/or in phase (Buryak et al., 2003; Rothenberg et al., 2002). In the case of amplitude optimization, the index modulation amplitude of the sampling was optimized following a Fourier analogy (Ibsen et al., 1998). In the case of phase-only optimization, only the relative phase of the channels to be generated are continuously modified and the amplitude modulation of the sampling is minimized. Such an approach was first demonstrated with semiconductor laser Bragg reflectors (Ishii et al., 1993) and it was recently applied to FBG (Rothenberg et al., 2002). Although this method can generate as many as 51-channel filters, phase-variation is still difficult to inscribe, requiring a customized lithographically prepared phase mask or a high precision inscription technique.

There is therefore an important demand for optimization methods for the design of sampling patterns giving a desired reflectivity spectrum (Rothenberg et al., 2002). In addition, the method requires performing global optimization as it is observed that functionals have multiple

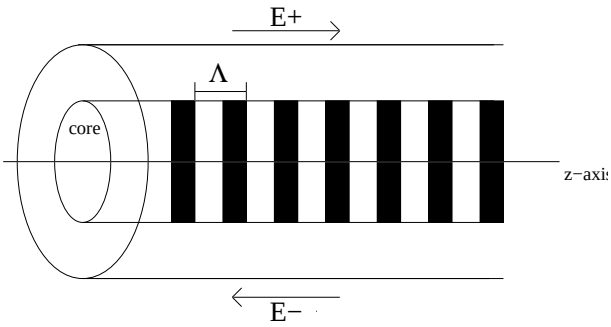

Figure 1: Fiber Bragg grating diagram: Dark stripes correspond to core zone where the refractive index is modulated. The fiber reflects a certain wavelength band, E-, and allows other one, E+, to pass. Λ represents the grating period.

minima (Skaar and Risvik, 1998).

In this paper we introduce a new global semi-deterministic optimization algorithm (SDA). The approach is compared to a well known genetic algorithm (Dumas et al., 2004; Goldberg, 1989) and applied to the design of FBG structures. We show that superior results can be found with this method from both industrial realizability and computational complexity point of view.

Section 2 presents the Fiber Bragg Grating devices and their mathematical modelling. Section 3 describes our optimization method and recalls the basis of genetic algorithms. Finally, in section 4 we discuss different designs of high-channel-count multichannel filters.

2 Fiber Bragg Gratings (FBG)

Fiber Bragg Gratings are based on the perturbation of the effective refractive index of an optical guide in order to reflect a predetermined wavelength band and to let other bands pass (see Figure 1). To write a FBG in an optical fiber, we expose it to UV Laser radiation. This radiation will modify the refractive index of the optical guide core in a periodic or an aperiodic way (Erdogan, 1997).

In order to derive a mathematical model of a FBG, we assume there exist only two counterpropagating guided modes in the FBG of respective amplitudes $A(z)$ and $B(z)$ for any wavelength λ in the transmission band. We denote by n_{eff} the unperturbed refractive effective index and by β the corresponding propagation constant. The perturbation by UV exposure, denoted by n_{eff}, of the refractive effective index along the fiber axis z is given by:

$$\delta n_{eff}(z) = \overline{\delta n_{eff}}(z)(1 + \nu \cos\left[\frac{2\pi}{\Lambda} z + \phi(z)\right]) \qquad (1)$$

where $z \in [-\frac{L}{2}, \frac{L}{2}]$, L is the fiber length, Λ is the nominal grating period, $\overline{\delta n_{eff}}(z)$ is the slowly varying index amplitude change over the grating (also called *apodization*), ν is the fringe visibility and $\phi(z)$ is the slowly varying index phase change (also called *chirp*).

While the modes are orthogonal in an ideal waveguide and therefore do not exchange energy, the presence of a dielectric perturbation causes the modes to be coupled. Introducing the detuning parameter:

$$\zeta = \beta - \frac{\pi}{\Lambda} = \frac{2\pi n_{eff}}{\lambda} - \frac{\pi}{\Lambda}$$

and the new unknowns:

$$R(z) = A(z)\exp(i\zeta z - \tfrac{\phi(z)}{2})$$
$$S(z) = B(z)\exp(-i\zeta z + \tfrac{\phi(z)}{2})$$

the coupled equations can be written as:

$$\frac{dR}{dz}(z) = i\hat{\sigma}(z)R(z) + i\kappa(z)S(z) \qquad (2)$$

$$\frac{dS}{dz}(z) = -i\hat{\sigma}(z)S(z) - i\overline{\kappa}(z)R(z) \qquad (3)$$

When δn_{eff} is small compared to n_{eff}, the two coupling coefficients can be approximated by:

$$\hat{\sigma}(z) = \zeta + \sigma(z) - \frac{1}{2}\frac{d\phi}{dz}(z) = \zeta + \beta\frac{\overline{\delta n_{eff}}(z)}{n_{eff}} - \frac{1}{2}\frac{d\phi}{dz}(z)$$

and

$$\kappa(z) = \frac{\nu}{2}\sigma(z)$$

σ is called the 'dc' (demi coupling) and κ the 'ac' (associated coupling) coefficient. This system known as the two modes coupling model is completed by the following boundary conditions:

$$R(-\frac{L}{2}) = 1 \qquad (4)$$

(the forward-going wave is incident from $-\infty$) and

$$S(\frac{L}{2}) = 0 \qquad (5)$$

(there is no backward-going wave for $z \geq \frac{L}{2}$).

The main characteristics of a FBG is then expressed through its complex spectral response in the transmission band:

$$\lambda \in [\lambda_{min}, \lambda_{max}] \mapsto \rho(\lambda) = \frac{S(-\frac{L}{2})}{R(-\frac{L}{2})} \qquad (6)$$

from which we deduce its power reflection function:

$$\lambda \in [\lambda_{min}, \lambda_{max}] \mapsto r(\lambda) = |\rho(\lambda)|^2 \qquad (7)$$

2.1 Uniform FBG

If the grating is uniform along z, then the apodization $\overline{\delta n_{eff}}$ and the chirp ϕ are constant functions, as well as κ and σ. Thus, equations (2-3) reduce to a system of first-order coupled ordinary differential equations with constant coefficients.

More precisely, the complex spectral response and the power reflection function can be approximated by the following expressions (see (Skaar and Risvik, 1998)):

$$\rho(\lambda) = \frac{-\kappa \sinh(\omega L)}{\hat{\sigma}\sinh(\omega L) + i\sqrt{\kappa^2 - \hat{\sigma}^2}\cosh(\omega L)} \quad (8)$$

and

$$r(\lambda) = \frac{\sinh^2(\omega L)}{\cosh^2(\omega L) - \frac{\hat{\sigma}^2}{\kappa^2}} \quad (9)$$

where $\omega = \sqrt{\kappa^2 - \hat{\sigma}^2}$.

2.2 Non-uniform FBG

Non-uniform apodization and chirped refractive index are suitable in applications. These permit a better reduction of undesirable sidelobes appearing in uniform FBG power reflection functions. For instance, a non uniform apodization of a FBG can eventually produce a power reflection function very close to the often desired "top-hat" shape.

In this case, the complex spectral response and the power reflection function are approximated by decomposing the FBG in a set of N uniform elementary fibers of length $\frac{L}{N}$. Expressions (8-9) are then used on each of these fibers to find the overall coefficients of the complete FBG. This leads to the so-called simplified transfer matrix method (Erdogan, 1997).

2.3 Non uniform sampled FBG

A sampled FBG is a superstructure made of a comb distribution of a sampling pattern. This is an efficient and simple technique to construct a grating that exhibits periodic maxima in its spectrum. Using the coupled mode theory (Erdogan, 1997), it can be shown that a spatial comb distribution leads to a comb of peaks with identical response and with a wavelength separation $\Delta\lambda$ varying as:

$$\Delta\lambda = \frac{2n_{eff}\Lambda^2}{P} \quad (10)$$

with P the period of the sampling patterns distribution. The computation of the reflectivity coefficients of a sampled FBG remains unchanged compared to the one exposed in the previous paragraph (Erdogan, 1997). But this calculation is more time-consuming.

2.4 The inverse problem of non uniform sampled FBG

In order to obtain a multi-channel filter, Ibsen et al. (Ibsen et al., 1998) have shown the possibility to inscribe inside the fiber core a Sinc-shaped apodization function (see Figure 3) with a continuous writing technique:

$$\overline{\delta n_{eff}}(z) = (\delta n_{eff})_{max} \frac{\sin(\frac{2N_l \pi z}{L})}{\frac{2N_l \pi z}{L}} \quad (11)$$

The number of secondary side loops of this function, $(2 * (N_l - 1))$, being proportional to the total number of targeted channels, a 16-peak filter was demonstrated with a profile exhibiting 14 secondary side loops between the main lobes. To physically express the negative values of the Sinc function, discrete π-phase shifts (or equivalently sign changes in the profile) were inserted between each side loop. However, this type of profile suffers several drawbacks. A great number of π-phase shifts must be inserted as the number of channels increases, which requires mastering the writing process. Moreover, as the number of channels increases, the duty cycle (i.e. the ratio between the central lobe and the rest of the grating) decreases proportionally to $\frac{1}{N}$. Most of the energy deposited onto the fiber finally concerns the writing of the central lobe so that the strength of reflectivity of the grating strongly decreases. In this way, a 16-channel count FBG with a reflectivity of 0.95 requires a maximum index variation up to 6.10^{-4}. Such values are impossible to realize in practice. In addition, using highly photosensitive fibers gives rise to a nonlinear regime during the UV-writing. All this makes it important to find profiles easier to implement by optimization.

3 Optimization methods

We propose to use two types of minimization methods. A typical genetic algorithm (Dumas et al., 2004; Goldberg, 1989) and a new global minimization method based on a recursive search for the attraction basins of any local optimization algorithm.

3.1 Genetic algorithm

Consider the minimization of a real functional $J(x)$, $x \in \Omega_{ad}$, x is the optimization parameter and belongs to an admissible space Ω_{ad}. Genetic algorithms approximate the global minimum (or maximum) J through a stochastic process based on an analogy with the Darwinian evolution of species:

- A family $(x_i)_{1 \leq i \leq N_p}$ of N_p possible solutions of the optimization problem, called 'individuals', is first randomly created in the search space Ω_{ad} in order to constitute the first generation of the 'population'.

- Each individual, representing a potential solution of the given problem, is ranked relatively to its associated value through an auxiliary "fitness" function (inversely proportional to J in the case of a minimization problem). In this process (selection process), better individuals, in terms of the fitness function, have higher chances to be chosen for reproduction.

- The next generation is then made from the current generation by creating 'offsprings' (crossover process) from different pairs of individuals; the offsprings may in turn eventually "mute" (mutation process).

With these three basic evolution processes, it is generally observed that the best obtained individual is getting closer after each generation to the optimal solution of the problem (Goldberg, 1989; Dumas et al., 2004). In practice, as final convergence is difficult with GA based algorithms, one should always complete GA iterations by a descent method for better accuracy, these approaches are called '*hybrid algorithms*'.

Engineers like GA's because these do not require sensitivity computation, perform global and multi-objective optimization and are easy to parallelize. Their drawbacks remain their weak mathematical background, their computational complexity and their lack of accuracy. The semi-deterministic algorithm (SDA) presented below aims to address these issues.

3.2 Semi-deterministic multi-level optimization

We want to minimize a functional $J : \Omega \to \mathbb{R}$ (where Ω is a subset of $\mathbb{R}^n$) subject to the following hypotheses (Mohammadi and Saiac, 2002): $J \in C^1(\Omega, \mathbb{R})$ and is coercive (i.e. $J(x) \to +\infty$ when $|x| \to +\infty$ in Ω). The minimum of J is denoted J_m. In cases where J_m is unknown, we set $J_m = 0$ and look for the best solution for a given complexity and computational effort.

The general idea of the Semi Deterministic Algorithm (SDA) is to improve the efficiency of any particular local deterministic minimization algorithms (Gradient, Newton, etc...), by making it global. It is based on a recursive search for the attraction basins of the local algorithm. For the sake of simplicity, we will only consider here the following optimal descent algorithm with an output called $D(x_0, I, \epsilon)$:

- **Input:** x_0, I, ϵ
- $x^1 = x_0$

For n going from 1 to I

- Determine $\rho_{opt} = argmin_\rho(J(x^n - \rho \nabla J(x^n)))$ using dichotomy
- $x^{n+1} = x^n - \rho_{opt} \nabla J(x^n)$
- **If** $J(x^{n+1}) < J_m + \epsilon$ **EndFor**

EndFor

- **Output:** $D(x_0, I, \epsilon) = x^{n+1}$

Above the inputs $x_0 \in \Omega$, $\epsilon \in \mathbb{R}$ and $I \in \mathbb{N}$ are respectively the initial condition, the stopping criterion and the iteration number.

We consider that the minimization problem is solved if the initial condition x_0 lies in the attraction basin of the global minimum of J. In order to determine such an initial condition, we consider $x_0 = v$ as a new variable in the previous algorithm to be found by the minimization of:

$$h(v) = J(D(v, I, \epsilon)) - J_m \tag{12}$$

To perform the minimization of (12), we then consider the following algorithm with an output called $A_1(v_1, N, I, \epsilon)$:

- **Input:** v_1, N, I, ϵ
- v_2 chosen randomly

For i going from 1 to N

- $o_i = D(v_i, I, \epsilon)$
- $o_{i+1} = D(v_i + 1, I, \epsilon)$
- **If** $J(o_i) = J(o_{i+1})$ **EndFor**
- **If** $min\{J(o_k), k = 1, ..., i\} < J_m + \epsilon$ **EndFor**
- $v_{i+2} = v_{i+1} - J(o_{i+1}) \frac{v_{i+1} - v_i}{J(o_{i+1}) - J(o_i)}$

EndFor

- **Output:** $A_1(v_1, N, I, \epsilon) = argmin\{J(o_k), k = 1, ..., i\}$

Above the inputs are $v_1 \in \Omega$, $(N, I) \in \mathbb{N}^2$ and $\epsilon \in \mathbb{R}$.

As this line search minimization algorithm might fail, an external level to the algorithm A_1 is added in order to have a multidimensional search. As previously, we consider $v_1 = w$ as a new variable in A_1 to be found by the minimization of:

$$\tilde{h}(w) = h(A_1(w, N, I, \epsilon)) \tag{13}$$

To perform the minimization of (13), we then consider the following two-level algorithm with an output called $A_2(w_1, M, N, I, \epsilon)$:

- **Input:** w_1, M, N, I, ϵ
- w_2 chosen randomly

For i going from 1 to M

- $p_i = A_1(w_i, I, \epsilon)$
- $p_{i+1} = A_1(w_i + 1, I, \epsilon)$
- **If** $J(p_i) = J(p_{i+1})$ **EndFor**
- **If** $min\{J(p_k), k = 1, ..., i\} < J_m + \epsilon$ **EndFor**
- $w_{i+2} = w_{i+1} - J(p_{i+1}) \frac{w_{i+1} - w_i}{J(p_{i+1}) - J(p_i)}$

EndFor

- **Output:** $A_2(w_1, M, N, I, \epsilon) = argmin\{J(p_k), k = 1, ..., i\}$

Above $w_1 \in \Omega$, $(M, N, I) \in \mathbb{N}^3$ and $\epsilon \in \mathbb{R}$. In order to add search directions, the previous construction can be easily pursued recursively.

The choice of the initial condition w_1 in this algorithm contains the only non-deterministic feature of the SDA method. In practice we randomly choose the initial condition $w_1 \in \Omega$ and we consider $(N, M, I) = (5, 5, 10)$. These values give a good compromise between computation complexity and result accuracy. Mathematical background for this approach and validation on academic test cases are available (Mohammadi and Saiac, 2002; Debiane et al., 2004).

4 Optimization problem

The GA and the SDA algorithms above are applied to solve the inverse problem of sampling pattern design of high-channel-count multichannel filters. We exhibit designs of

100 mm long multichannel filters centered around 15525 nm that consist of 16 and 38 totally reflective identical channels spaced 100 GHz. We discuss their spectral characteristics and compare them to the responses obtained with currently used Sinc-profiles.

4.1 Cost function

We design a sampled FBG knowing its power reflection function (7). We can reformulate this problem considering that each sampled FBG with no chirp can be characterized by its apodization (or equivalently refractive index modulation) $z \mapsto \overline{\delta n_{eff}}(z)$, we denote by Ω_{apo} the associated search space of all acceptable apodization profiles. The functional is given by:

$$J(x) = \|r(x) - r_{target}(x)\|_{L^2([\lambda_{min},\lambda_{max}])} \tag{14}$$

where $r(x)$ is the power reflection function of the sampled FBG with an apodization associated with $x \in \Omega_{apo}$ and $r_{target}(x)$ the nearest perfect power reflection function to $r(x)$ matching the desired requirements.

4.2 Parameterization

In order to find a multi-channel filter with the desired spectral response and associated with an index modulation with some 'interesting' characteristics (smooth enough, slowly varying and symmetric), apodization profiles are generated by spline interpolation through a reduced number of N_S points equally distributed along the first half of the sampling pattern and completed by parity. We will choose a value of N_S high enough to ensure a large number of peaks in the spectral response but small enough to ensure improvement in the index modulation profile in comparison with the classical Sinc profile. Thus, the corresponding search space of the optimization problem is a hypercube:

$$\Omega_{N_S} = [-\overline{n}_{max}, \overline{n}_{max}]^{N_S} \tag{15}$$

where $\overline{n}_{max}$ is a design constraint. Here $\overline{n}_{max} = 5.10^{-4}$.

The functional on Ω_{N_S} is defined by:

$$J_{N_c}(x) = \sum_{i=1}^{N_c} (r(x)(\lambda_i) - r_{target}(x)(\lambda_i))^2 \tag{16}$$

In the above expression, the power reflection function $r(x)$ of the filter with an apodization associated with $x \in \Omega_{N_S}$ is evaluated on N_c wavelengths equally distributed on the transmission band by using the simplified transfer matrix method (Erdogan, 1997). On the other hand, $r_{target}(x)$ denotes the nearest perfect power reflection function to $r(x)$ matching the desired requirements (see Figure 2), namely N_{peaks} transmitted wavelengths with a transmission rate greater than 0.95 and separated by $\Delta\lambda$:

$$r_{target}(x)(\lambda) = \begin{cases} \max(0.95, r(x)(\lambda)) \ if \ \lambda \in \Lambda \\ 0 \text{ elsewhere} \end{cases} \tag{17}$$

with $\Lambda = \{\lambda_x, \lambda_x + \Delta\lambda, \ldots, \lambda_x + (N_{peaks} - 1)\triangle\lambda\}$, λ_x being the lowest frequency peak and for $\lambda \in [\lambda_{min}, \lambda_{max}]$.

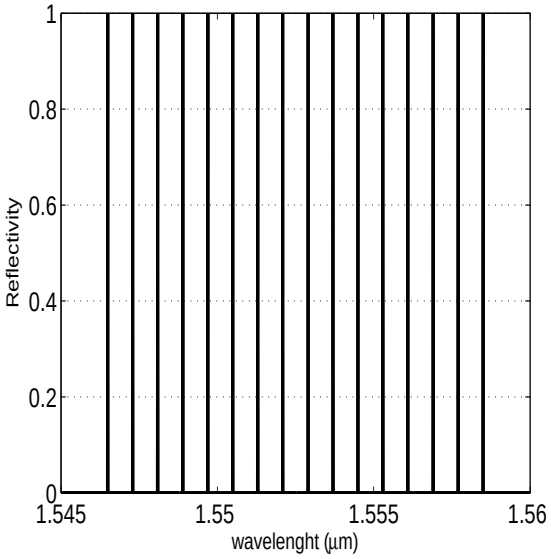

Figure 2: Example of ideal reflectivity for a 16-peak filter.

5 Results and discussion

Two different FBG configurations have been considered for optimization with GA and SDA algorithms above. The results have been compared to the empirical technique based on Sinc functions. The grating profile has been optimized on the entire length of a sampling period equal to 1.039 mm, corresponding to an interchannel spacing $\Delta\lambda = 0.8$ μm (10). The total length of the grating is set to 103.9 mm. The initial core effective refractive index is $n_0 = 1.45$.

For the genetic algorithm, we have chosen the following values for the three associated stochastic processes (see section 3.1). The crossover is barycentric in each coordinate with a probability of 0.45. The mutation process is non-uniform with a refinement parameter of 1.1 and probability of 0.15. The selection is a roulette wheel type proportional to the rank of the individual in the population. A one-elitism principle, that consists in keeping the best current individual in the next generation, has also been imposed. The population size has been set to 180 and the maximum generation number to 30.

For the semi-deterministic algorithm, we use a three-level structure with $M = N = 5$ iterations for the external levels and $I = 10$ iterations of conjugate gradient as core optimization method (calculations after doubling these numbers give rise to the same solutions). We see that the complexity in terms of calculation and memory requirement is quite low. These parameters are fixed and used in all computations.

5.1 Npeaks= 16, Ns=9, Nc=1200

Figures 3 and 4 show the apodization variation profile and the associated power reflection function between 1540 and 1560 μm for three different filters: Sinc, GA and SDA (i.e.

	Sinc	GA	SDA
J_{N_c} value	6.6	5.9	3.1
Evaluation number	$\cdots$	5400	3000
Out-of-band rejection	0.4	0.15	0.03
$\Delta\overline{n}_{max}$	5 10^{-4}	2.1 10^{-4}	1.9 10^{-4}
Phase shifts	14	6	4

Table 1: 16-peak multichannel filter: left to right, results with Sinc, GA and SDA apodization profiles.

obtained by these optimization procedures). The Sinc filter has a cost function of 6.59. The GA filter gives 5.83. The total number of functional evaluations is 5400 and the best element was found at generation 21 of GA after 3780 evaluations. The SDA filter gives 3.09. The total number of functional evaluations is about 3000. The best element was found at iteration 169 after 2028 evaluations. This is important as Sinc profiles are considered efficient and realistic for the realization of these filters. Convergence histories are given in Figure 5. The three values of the cost function show that both GA and SDA algorithms have led to better solutions in terms of reflection characteristics than the Sinc profile. This is visible in Figure 3 on the respective interchannel and out-of-band rejection (undesirable side peaks) which is reduced to 0.03 in the SDA profile and to 0.15 in the GA profile, to be compared to 0.4 for the Sinc profile. In addition, optimized profiles are more suitable for industrial realization as the number of necessary phase shifts (when $\overline{\delta n_{eff}}(z) = 0$) is only 6 for the GA profile and 4 for SDA against 14 for the Sinc-profile and the index modulation of profiles is more homogeneously distributed along the pattern and does not exhibit any dominant lobe. A last improvement concerns the maximum amplitude of the profile which has been reduced to $\Delta\overline{n}_{max} = 2.10^{-4}$ for both GA and SDA profiles. These results are summarized in Table 1.

5.2 Npeaks= 38, Ns=15, Nc=2400

In this case, the classical sinc-type profile exhibits better spectral characteritics than the SDA and GA optimized profiles as can be observed in Figures 6 and 7 or in the corresponding values of J_{N_c} (9.1 for sinc against 10.3 for SDA and 13.9 for GA). Furthermore, the GA optimized profile fails to exhibit all the 38 peaks with a reflection higher than 0.95. However, the sinc profile is difficult to build because of its large amount of phase shifts (36) and its large maximum index amplitude (6×10^{-4}). Actually, the SDA algorithm could have found results equivalent to, or better than, the sinc-type profile if a larger value N_s had been taken (e.g. $N_s > 40$). However, to avoid the above-mentioned experimental difficulty, we explicitly removed such unsuitable profiles with the choice of a reduced search space. Thus, the obtained FBG is easier to implement as the number of phase shifts is reduced to 14, the index modulation is more homogeneously distributed and the maximum amplitude of the profile is reduced to

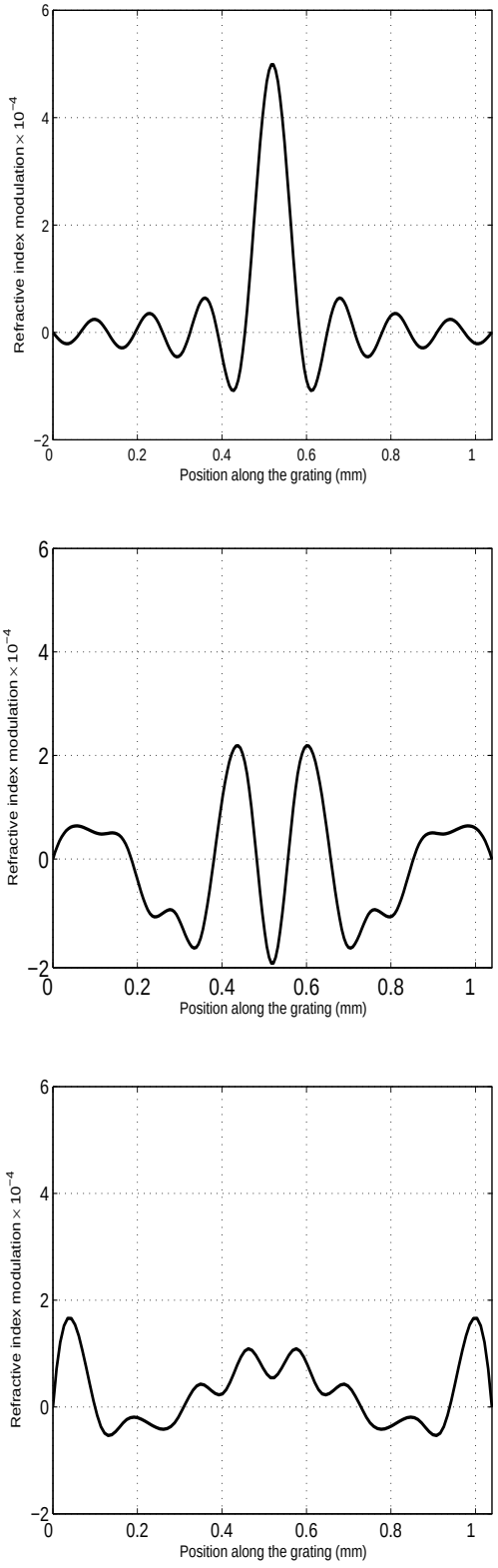

Figure 3: 16-peak multichannel filter. From top to bottom: SINC, GA and SDA optimized filters apodization.

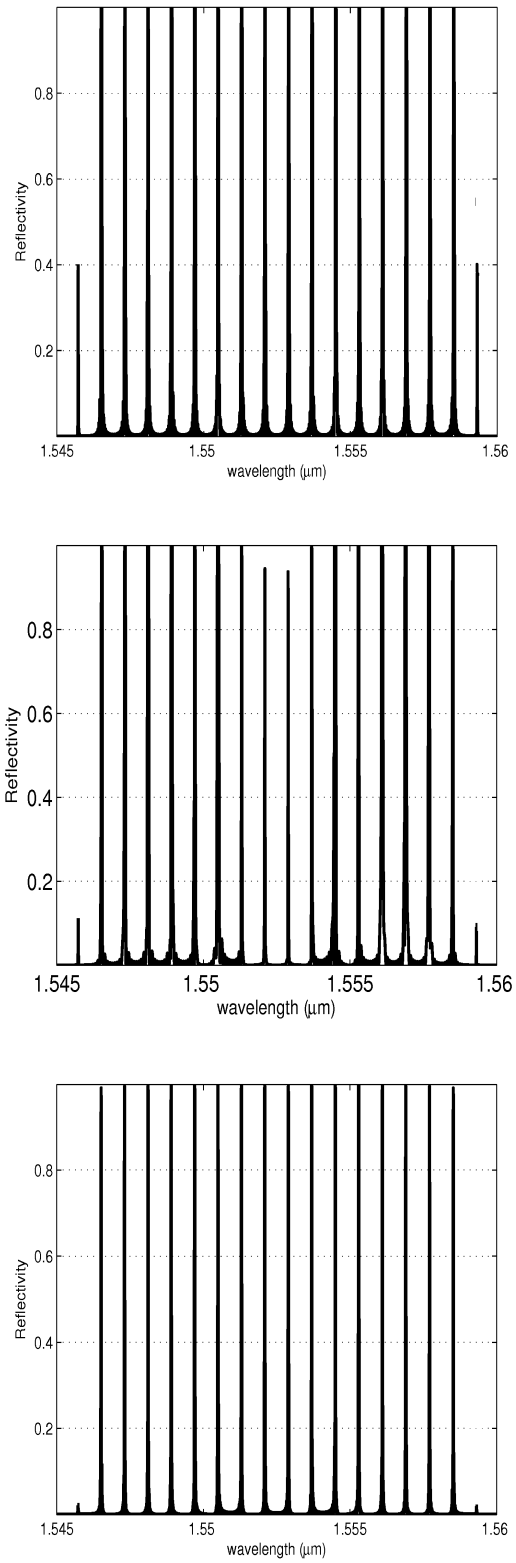

Figure 4: 16-peak multichannel filter. From top to bottom: Sinc, GA and SDA optimized filters associated spectra.

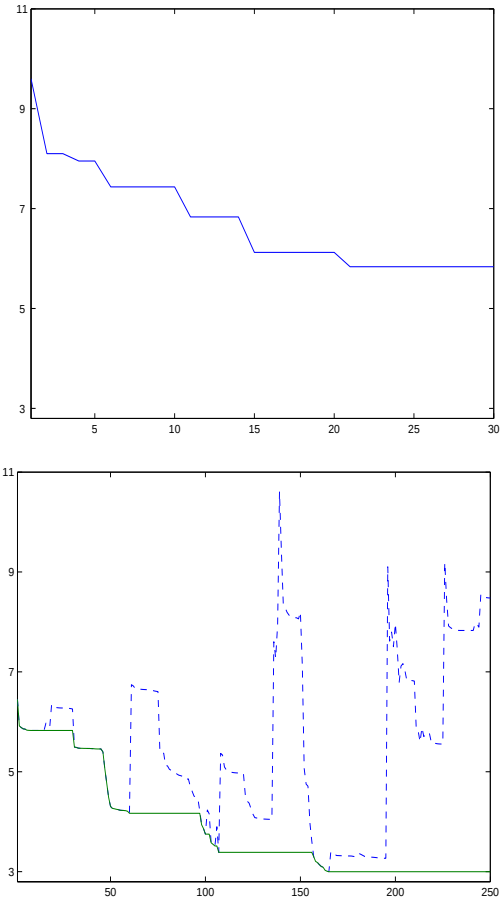

Figure 5: 16-peak multichannel filter. GA (**Left**) and SDA (**Right**) convergence histories: Best element (**solid line**) and global convergence (**dashed line**).

	Sinc	GA	SDA
J_{N_c} value	9.8	13.9	10.3
Evaluation number	$\cdots$	5400	4500
Peak number	38	34	38
$\Delta\overline{n}_{max}$	6 10^{-4}	3.5 10^{-4}	4.8 10^{-4}
Phase shifts	36	22	14

Table 2: 38-peak multichannel filter: left to right, results with Sinc, GA and SDA apodization profiles.

$\Delta\overline{n}_{max} = 4.8 \times 10^{-4}$ (see Table 2). The total number of functional evaluations is now 4500 for SDA and almost unchanged for GA at 5400. With GA, the best element is found at generation 28 after 5040 evaluations (almost at the end) while it is reached at iteration 89 after 1602 evaluations by SDA. This is visible in Figure 8.

6 Conclusion

Two configurations of high channel count filters based on non-chirped apodized fiber Bragg gratings have been

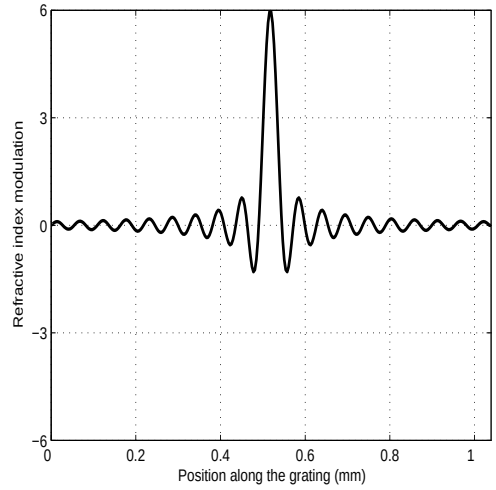

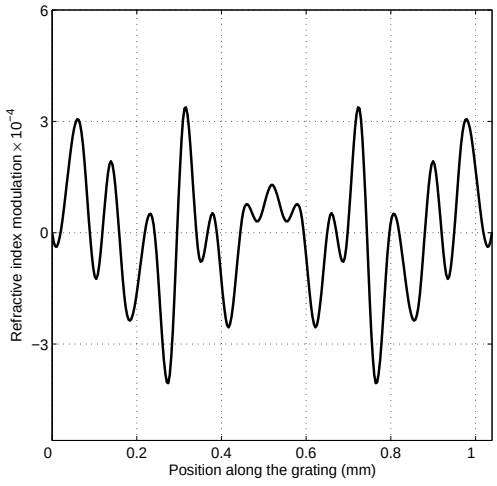

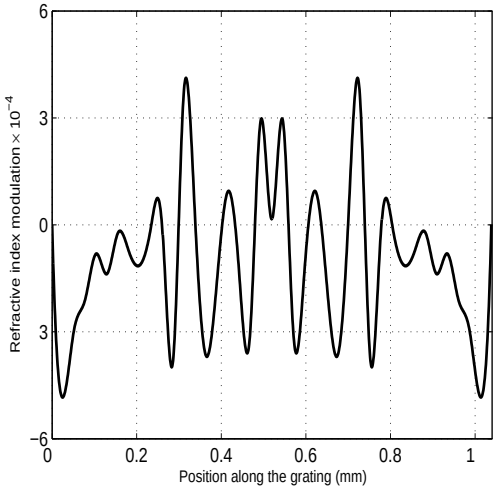

Figure 6: 38-peak multichannel filter. From top to bottom: SINC, GA and SDA optimized filters apodization.

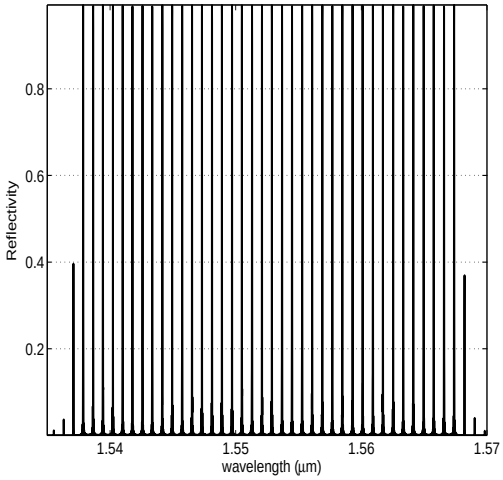

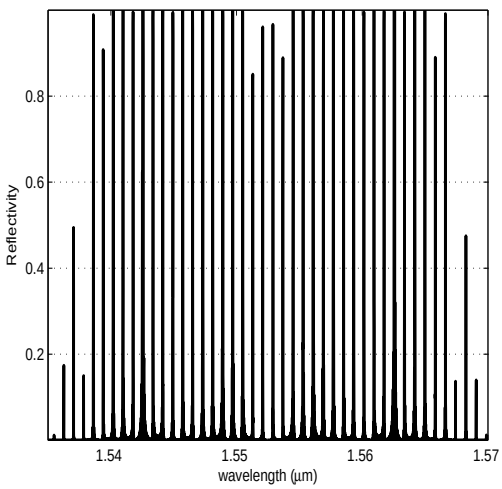

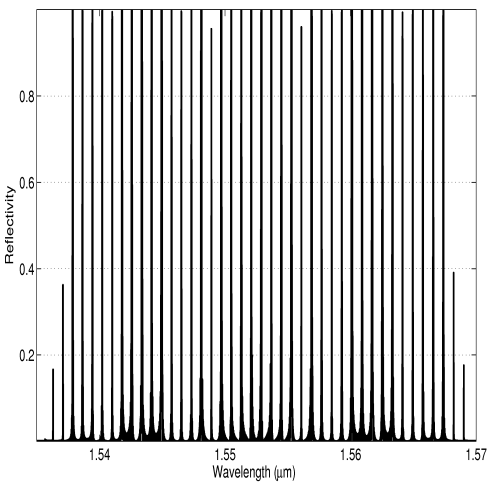

Figure 7: 38-peak multichannel filter. From top to bottom: Sinc, GA and SDA optimized filters associated spectra.

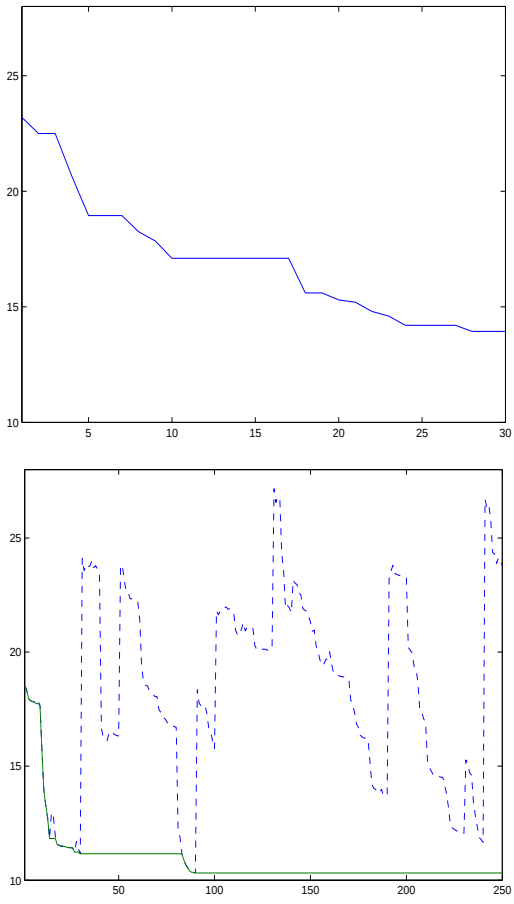

Figure 8: 38-peak multichannel filter. GA (**Top**) and SDA (**Bottom**) convergence histories: Best element (**solid line**) and global convergence (**dashed line**).

analyzed by global optimization methods using a semi-deterministic and a hybrid genetic optimization algorithm. This leads to the creation of four filters with different FBG apodization profiles. The results obtained by the semi-deterministic algorithm outmatch those by the genetic algorithm and also the sinc method traditionally used in industry.

The grating solutions produced by the semi-deterministic approach are easier to manufacture because they have no step variation, lower maximum index modulation value and also smaller number of π-phase shifts in the sampling pattern. A prototype of this fiber is developed by the Electronic and MicroOptoElectronic Center at Montpellier University.

Recently, this approach has been successfully extended to the design of Spectral Code Division Multiple Access (spectral CDMA) filter devices (Ivorra et al., 2004).

Acknowledgements

The authors would like to thank Professor Yves Moreau from the Electronic and MicroOptoElectronic center of the University of Montpellier (CEM2).

REFERENCES

Buryak, A.V., K.Y. Kolossovski and D.Y. Stepanov (2003), 'Optimization of refractive index sampling for multi-channel fiber bragg gratings', *IEEE Journal Quantum Electron.* **39**, 91–98.

Chow, J., G. Town, B. Eggleton, M. Ibsen, K. Sugden and I. Bennion (1996), 'Multiwavelength generation in an erbium-doped fiber laser using in-fiber com filters', *IEEE Photonic Technology Letter* **8**(1), 60–62.

Debiane, L., B. Ivorra, B. Mohammadi, F. Nicoud, A. Ern, T. Poinsot and H. Pitsch (2004), Temperature and pollution control in flames, *in* 'Proceeding of the Summer Program', Center for Turbulence Research, NASA AMES/Stanford University, USA, pp. 367–375.

Dumas, L., V. Herbert and F. Muyl (2004), 'Hybrid method for aerodynamic shape optimization in automotive industry.', *Computers and Fluids* **33**(5), 849–858.

Eggleton, B.J., P.A. Krug, L. Polodian and F. Ouellette (1994), 'Long periodic superstructure bragg gratings in optical fibres', *Electronic Letter* **30**(19), 1620–1622.

Erdogan, T. (1997), 'Fiber grating spectra', *Journal of LightwaveTechnology* **15**(8), 1277–1294.

Goldberg, D. (1989), *Genetic algorithms in search, optimization and machine learning.*, Addison Wesley.

Helmers, H., O. Durand, G.H. Duan, E. Gohin, J. Landreau, J. Jacquet and I. Riant (2002), '45 nm tunability in c-band obtained with external cavity laser including novel sampled fibre bragg grating.', *Electronic Letter* **38**(24), 1535–1536.

Ibsen, M., M.K. Durkin, M.J. Cole and R.I. Laming (1998), 'sinc-sampled fiber bragg gratings for identical multiple wavelength operation', *IEEE Photonic Technology Letter* **10**(6), 842–844.

Ishii, H., Y. Tohmori, Y. Yoshikuni, T. Tamamura and Y. Kondo (1993), 'Multiple-phase-shift super structure grating dbr lasers for broad wavelength tuning', *IEEE Photonic Technology Letter* **5**(6), 613–615.

Ivorra, B., B. Mohammadi, L. Dumas, Y. Moreau, G. Pille and O. Durand (2004), 'Apodisation de fibres à réseaux de bragg pour la synthèse de codes cdma spectral', *Conference COSTO04, IEEE Lasers and Electro-Optics Society French Chapter* .

Loh, W.H., F.Q. Zhou and J.J. Pan (1999), 'Novel designs for sampled grating-based multiplexers-demultiplexers', *Optics Letter* **34**(21), 1457–1459.

Mohammadi, B. and J-H. Saiac (2002), *Pratique de la simulation numérique*, Dunod.

Rothenberg, J.E., H. Li, Y. Li, J. Popelek, Y. Sheng, Y. Wang, R.B. Wilcox and DJ. Zweiback (2002), 'Fiber bragg gratings and phase-only sampling for high channel counts', *IEEE Photonic Technology Letter* **14**(9), 1309–1311.

Skaar, J. and K.M. Risvik (1998), 'A genetic algorithm for the inverse problem in synthesis of fiber gratings.', *Journal of Lightwave Technology* **16**(10), 1928–1932.

Wei, D., T. Li, Y. Zhao and S. Jian (2000), 'Multiwavelength erbium-doped fiber ring lasers with overlap-written fiber bragg gratings', *Optics Letter* **25**(16), 1150–1152.